Efficient separation of precious metals from computer waste printed circuit boards by hydrocyclone and dilution-gravity methods

Downloaded from: https://research.chalmers.se, 2026-04-07 05:37 UTC

Citation for the original published paper (version of record):
Bilesan, M., Makarova, I., Wickman, B. et al (2021). Efficient separation of precious metals from computer waste printed circuit boards by
hydrocyclone and dilution-gravity methods. Journal of Cleaner Production, 286.
http://dx.doi.org/10.1016/j.jclepro.2020.125505

N.B. When citing this work, cite the original published paper.

research.chalmers.se offers the possibility of retrieving research publications produced at Chalmers University of Technology. It covers all kind of research output: articles, dissertations, conference papers, reports etc. since 2004. research.chalmers.se is administrated and maintained by Chalmers Library

(article starts on next page)

Journal of Cleaner Production 286 (2021) 125505

Contents lists available at ScienceDirect

Journal of Cleaner Production

journal homepage: www.elsevier.com/locate/jclepro

Efficient separation of precious metals from computer waste printed circuit boards by hydrocyclone and dilution-gravity methods

Mohammad Reza Bilesan [a, *], Irina Makarova [a], Björn Wickman [b], Eveliina Repo [a]

[a] Department of Separation Science, LUT University, FI, 53850, Lappeenranta, Finland
[b] Department of Physics, Chalmers University of Technology, 412 96, Gothenburg, Sweden

ARTICLE INFO

Article history:
Received 22 June 2020
Received in revised form
5 December 2020
Accepted 9 December 2020

Handling editor: Cecilia Maria Villas Bôas de Almeida

Keywords:
Waste printed circuit board
Hydrocyclone
Gravity method
Precious metals
Rosin-Rammler-Bennett model

ABSTRACT

To fulfill the different aspects of green chemistry and to achieve full use of the secondary resources (waste printed circuit boards (WPCB)), the necessity of developing green methods for recovery of precious metals (Au, Pd, and Ag) is highly demanded. In this study, a novel environment-friendly physical separation approach; the combination of crushing, grinding, sieving as pretreatment steps alongside hydrocyclone and the dilution-gravity method (DGM) as the main final steps; is proposed. Inductively coupled plasma-mass spectrometry (ICP-MS), atomic absorption spectroscopy (AAS), and energy-dispersive X-ray spectroscopy (EDS) characterization methods were utilized to understand the effects of different separation steps applied in this research. The size and shape of grinded materials and the ones produced after hydrocyclone and DGM were evaluated using scanning electron microscopy. The results showed that the sieving step separated the highest gold fraction in the finer classification (<75 μm) while placed the copper (70 wt.%) into the coarser contents. The overflow to underflow outlet diameter ratio and inlet pressure was evaluated to determine the separation efficiency of a hydrocyclone effect of parameters. In the best-case scenario at 3 bar hydrocyclone operation pressure where the overflow to underflow outlet diameter (Do/Du) was 6.5, the highest metal fraction (87 wt.%) was achieved in the sink of the DGM. In this case, the total separation efficiency of gold, palladium, silver, and copper was 75%, 78%, 64%, 72%, respectively. Thus, this study demonstrates the feasibility of utilizing the sieving as mentioned above classification pretreatment steps followed by hydrocyclone and DGM methods as promising approaches for recovering precious metals from WPCBs that contain annually almost 50 million tons of e-waste.
© 2020 The Author(s). Published by Elsevier Ltd. This is an open access article under the CC BY-NC-ND license (http://creativecommons.org/licenses/by-nc-nd/4.0/).

1. Introduction

End-of-life printed circuit boards are one of the fastest-growing e-waste streams which pose potential environmental and health threats. Furthermore, due to the significant quantity of precious metals in circuit boards, finding the most effective and affordable separation method to separate the valuable metals is increasingly important to eradicate e-waste piling up in the landfills. E-waste generation is estimated to be approximately 50 million tons of e-waste per annum (Ruediger K., 2011; Huisman J., 2012). The recycling of e-waste improves supply chain sustainability and support a circular economy. Mainstream metals refining corporations are currently exploiting profits from e-waste and touting for business. High client demand for the newest and most powerful gadgets leads to increasing electronic device production. Therefore, less sophisticated techniques tend to be used for recovering metals (Purchase, D., 2020), which have harmful implications for both labor safety and the environment. These activities, which involve landfills and factories can threaten public health and ecosystems seriously. Furthermore, the implementation of efficient processes and feasible techniques is essential in valuable metals recovery from e-waste, and new and improved techniques for increased efficiency of e-waste recycling are highly sought after.

The average values of selected material composition in Waste Printed Circuit Boards (WPCBs) are presented in Table 1.

Generally, the non-metal fraction (NMF) of WPCBs represents approximately 70% of the mass of the WPCB. The NMF consists of fiberglass or cellulose as reinforcing materials (3%), EPDM (0.9%), epoxy, and phenolic or polyester as resins (3%). The most common types of WPCBs are etain (3.9%), polyethylene (2.1%),

* Corresponding author.
E-mail address: Mohammad.Reza.Bilesan@lut.fi (M.R. Bilesan).

https://doi.org/10.1016/j.jclepro.2020.125505
0959-6526/© 2020 The Author(s). Published by Elsevier Ltd. This is an open access article under the CC BY-NC-ND license (http://creativecommons.org/licenses/by-nc-nd/4.0/).

Table 1
Material composition of Printed Circuit Boards (PCBs).

Materials	Element	Vasile et al. (2008)	Hino et al. (2009)	Birloaga et al. (2013)	Yang et al. (2009)	Oishi et al. (2007)	Behnamfard et al. (2013)	Fogarasi et al. (2014)	Gramatyka et al. (2007)	Cui and Zhang (2008)	Average
Organic epoxy resin	C(wt.%)	24.7	18.1	–	–	–	–	–	–	–	21.4
	H(wt.%)	1.38	1.8	–	–	–	–	–	–	–	1.6
	N(wt.%)	0.85	0.32	–	–	–	–	–	–	–	0.6
	Br(wt.%)	4.94	5.07	–	–	–	5.88	–	–	–	5.3
	Sb(wt.%)	–	0.45	–	–	0.16	0.37	–	–	–	0.3
Inorganic glass fiber	–	–	37.6	–	–	–	–	–	–	–	37.62
Elements	Cu(wt.%)	13.8	14.6	30.6	25.1	26	19.2	18	20.12	14.3	20.2
	Fe(wt.%)	1.97	4.79	15.21	0.66	3.4	1.13	3	8.11	4.5	4.8
	Sn (wt.%)	–	5.62	7.36	1.86	4.9	0.69	4	4	–	4.1
	Ni(wt.%)	0.17	1.65	1.58	0.0024	1.5	0.17	1.11	2	1.1	1.0
	Zn(wt.%)	–	–	1.86	0.04	2.6	0.84	1.71	1	–	1.3
	Pb(wt.%)	–	2.96	6.7	0.8	3	0.39	2.31	2	2.2	2.5
	Au(ppm)	–	205	238	–	–	130	110	100	566	224.8
	Ag(ppm)	–	450	688	–	630	704	180	200	639	498.7
	Pd(ppm)	–	220	–	–	–	27	–	100	124	117.8

polypropylene, polyesters, and polycarbonates (6.9%), PVC (6%), and ABS (4.2%) are typical plastic components (Guo et al., 2009). The rest of the constituents are silicon, bismuth, beryllium, calcium, and magnesium oxides (Tiwary et al., 2017). On the other hand, WPCBs are an essential source of base and precious metals providing an economic incentive for their recycling (Lehner T., 1998; Bleiwas D. and Kelly T., 2001; He et al., 2006; Deveci H. et al., 2010). The average metal content in WPCBs is approximately 30–35% (Vasile C. et al., 2008; Birloaga I. et al., 2013; Oishi T. et al., 2007; Fogarasi S. et al., 2014).

Most of the inorganic materials included in PCBs are reported to the density range of 1.55–19.3 g/cm^3. WPCBs contain various valuable metals such as copper, silver, gold, and palladium. Furthermore, the different density characteristics of the elements in PCBs can be taken into consideration for the separation of non-metals and precious metals. As gold especially has the highest density among the other elements, gravity methods can provide the best selective separation for the gold (Gray, T., 2012).

Due to the mutual challenges regarding the e-waste recycling, it is necessary to design the new methods for the recovery of metals. On the one hand, according to the newest designs of Gigabyte and Asus [1, 2] in their future PCBs, a higher amount of precious metals is being used to upgrade desired features of the electronic and electric boards' demands. On the other hand, to recover the valuable metals, hazardous materials such as lead and flame retardant bearing chemicals require pretreatment before proper disposal (Kumar A. et al., 2018). China, India, and South Africa, which are the traditional destination of the global e-waste, have introduced new strict regulations in terms of importing e-wastes (Guarnieri P., 2020; Goodship V., 2019; Zhang S., 2015). While there are many challenges for e-waste recycling and exporting, the most effective way to solve the problem is to develop an affordable and more environmentally friendly recycling technology to ease the burden of e-waste recycling for industry. However, it is worth mentioning that precious metals extraction from virgin-mines is struggling with the technology and environmental challenges. For instance, the gold concentration in ores to be mined can be as low as 0.4 g/t and it is more complicated to concentrate the content (Lee J. C. and Srivastava R. R., 2016). Furthermore, highly toxic chemicals such as cyanide are required to recover the gold. Therefore, e-waste recycling will bring a reasonable point to be considered as the primary precious metals' mines.

There are different physical and mechanical recycling techniques for e-waste treatment. The following separation steps use cyclone, fluidization, or jigging as the separation method (He W. et al., 2006; Xue M. et al., 2012; Barnwal A. et al., 2020; Zhu X. N. et al., 2020, Cui J., and Forssberg E., 2003). These methods include different pretreatment steps such as dry crushing and pulverizing to obtain a mixture of metal and non-metal components. Magnetic separation to extract ferrous particles, eddy current, and high voltage electrostatic separators to separate the metal constituents are also utilized (Xue M. and Xu Z., 2013; Duan C. et al., 2009; Le et al., 2014; Ilyas S. et al., 2014). Regarding the feasibility of the requirements, technologies can be combined into one unit section with automated lines for e-waste recycling (Zhou L. et al., 2012; Duan et al., 2009). However, applying pretreatment before mechanical and physical separations affects the cost of the separation processes. In addition, the previous mechanical and physical studies encounter with some issues, for instance, agglomeration of fine particles during cyclone and fluidization. Regarding the gravity separation methods, as the particle size is reduced (<100 μm), the water flow becomes dominant over the centrifugal force therefore the gravity separation of fine particles could not be effective (Murthy Y. R. et al., 2011; Barnwal A. et al., 2020). In fluidization, the collector requirements such as ionic collectors (oil) to separate hydrophobic and hydrophilic materials will add further organic removal steps for powders, which are used for highly sensitive electrochemical recovery methods.

The significant complex, layered design of WPCBs makes it complicated to achieve an efficient separation by so-called jigging process whereas the leading force is used oscillation by the pulsing of water through the material that allows separate suspension into layers according to different densities (the heaviest concentrate forming the lowest layer and the lightest product the highest one). The negative point of this technique is the impossibility of dividing particles less than 1 mm in size (Schubert G, 1991). In addition to the abovementioned pretreatment methods, thermal treatment and pyrolysis are presented as thermal recycling techniques, which are considered as the supplementary procedure to achieve extra non-metals separation (Fujita T. et al., 2014). According to the most

recent studies, high temperatures up to 800 °C have been considered to eradicate the toxic compounds emissions in separation procedures, and purifying the metals' values (Barnwal A. et al., 2020; Nie C.C. et al., 2020; Hossain et al., 2018; Shokri et al., 2017; Ulman et al., 2018a, 2018b). However, besides high energy consumption, it is acknowledged that the different heating steps can lead to removing Au contents in the solder films. Regarding the equilibrium diagram phase, at the temperature of 250 °C, a two-phase of 63Sn−37Pb matrix and $AuSn_4$ intermetallic compound can be formed (Vianco P.T. et al., 1996, 1993). Therefore, the introduction of a viable method without thermal treatment is of paramount for WPCBs' recycling. Comparison of different approaches about recycling of WPCBs are presented in Table 2.

Motherboards were used as an object of research, whereas printed circuit boards can be collected either from other secondary resources. It can be noticed that even in one form of PCBs, for instance, motherboards, the amount of precious metals varied considerably through the years. In particular, gold values above 1000 ppm were reported in 1993 and 1995. Since then, all values have been reported are below 1000 ppm, with most values below 100 ppm (Bizzo W.A. et al., 2014). Therefore, considerable differences in the composition of collected PCBs should be considered in recycling techniques. Similar types of PCBs provide more homogeneous material to the mixtures of different e-wastes.

This work aims to define the leading affordable and more straightforward strategies for the separation of valuable metals and the non-metal fraction (NMF) from e-waste based on the dilution-gravity method (DGM) combined with a hydrocyclone. All the WPCBs' powders are controlled by water flow during the separation process. Hydrocyclone was chosen as a feasible method that was successfully applied for separation of plastic waste (Gent M. et al., 2018; Fu S. et al., 2019). However, to the best of authors' knowledge separation of WPCBs have not been studied extensively by hydrocyclone. The milling and sieving steps were considered as the first vital steps to concentrate the valuable components. On the one hand, it was expressed previously that fine particles are challenging for the hydrocyclone method as lower efficiencies can be obtained (Vieira, L.G. and Barrozo, M.A., 2014). On the other hand, the finer particle size distribution is vital for enhancing the recovery steps. Consequently, the optimal operating configurations of the hydrocyclone were investigated. The hydrocyclone technique is a simple design, it has high reliability, and uses low maintenance equipment which is required to separate uniform shapes, sizes, and higher density of precious metals. In addition, the dilution-gravity method (DGM) is considered as a simple, efficient method combined with hydrocyclone. The process was evaluated by inductively coupled plasma-mass spectrometry (ICP), atomic absorption spectroscopy (AAS), scanning electron microscope (SEM), and energy-dispersive x-ray spectroscopy (EDS) analysis. The Rosin-Rammler-Bennett (RRB) model was used to evaluate the separation characteristics of the particle size distribution results obtained by particle size analyzer. Therefore, this study design is based on a simple, environmentally friendly method with the advantage of low toxic dust dispersion.

2. Materials and methods

2.1. Materials and sample preparation

Disassembled printed circuit boards (motherboards) from end-of-life computers (manufactured between 1998−2010, LUT University, Finland) were cut into pieces of 30 mm × 30 mm by a Hand Guillotine Shear Cutter. Further, the comminuted parts were milled to 0.25 mm grain size using a cross beater mill (Retsch, SK 300, Germany) with a rotating speed of 3000 min^{-1} to fragment the components. The sieving step was performed by using a sieve shaker (Horizontal Sieve Shaker AS 400 Control, Retcsh, Germany) to classify powder based on the grain size. The samples were divided into five different size fractions. The set of sieves was 200, 150, 100, and 75 μm.

2.1.1. Hydrocyclone separation method

In the first step of separation procedure, a Richard Mozley Limited (Redruth, UK) hydrocyclone (Fig. 1) was utilized to separate valuable metals through a continuous classification of solid particles according to their different size, shape, and density characteristics (Bai et al., 2009b; Ghadirian et al., 2015). Hydrocyclone consists of a cylindrical section at the top and a conical base. In this method, the suspension is fed through a tangential inlet to generate a centrifugal field by a downward helical vortex inclining close to the wall of the hydrocyclone. The vortex approaches the underflow outlet when a reverse helical flow in the axial direction towards the vortex finder is generated. The vortex finder is a tube positioned axially from top of the hydrocyclone towards the lower edge of the suspension entry. The coarse and high dense particles in the feed stream are directed to the underflow outlet (Cilliers J. J, 2000; Cullivan et al., 2004; Svarovsky, 2000).

The overflow diameter was 14.3 mm, the cone angle 7°, and the column thickness 5 mm. The hydrocyclone separation procedure was accomplished in different overflow (OF) to underflow (UF) diameter ratio (Do/Du) at different feed inlet pressure over the range of 1−3 bar. The details of the performed experiments are presented in Table 3. In order to change the Do/Du ratio, the underflow diameter was altered over the range of 1.5−5 mm while the overflow diameter (14.3 mm) was kept constant. Particle size lower than 75 μm was selected due to the highest fraction of precious metals in this sieved portion. Moreover, lower particle size will enhance the leaching efficiency (Sun et al., 2018) during the chemical/electrochemical recovery of valuable constituents which can be considered for the future research. Therefore, the suspension of 120 g motherboard powders with particle size lower than 75 μm dispersed into 10 L of water was used for each experiment (Svarovsky L., 2000; Gonçalves et al., 2017). In order to minimize the effect of particles' agglomeration, all the suspensions were thoroughly mixed at the stirring rate of 1000 rpm. In each set of experiments, at first the hydrocyclone was set to the desired pressure and the suspension was recirculated for 15 min to stabilize the system, and to achieve a homogenized suspension. Thereafter, the samples were taken from both overflow and underflow simultaneously at a defined constant time. The same procedure was applied for different Do/Du ratios.

2.1.2. Dilution-gravity method

In the next step, the dilution-gravity separation (DGM) (Ren Y. et al., 2017) of underflow samples from the hydrocyclone step was performed. In the DGM, the underflow suspended solution was initially transferred into clean glass beaker and diluted by ultrapure water until 1000 mL (Fig. 1). Thereafter, the diluted suspension was mechanically stirred with a propeller stirrer at 500 rpm at 22 °C for 5 min. Afterwards, 900 mL of supernatant including float sample was transferred to another beaker and subsequently filtered using a Buchner system and Whatman paper (grade 42 filter paper whatman®, UK). The rest of the solution (100 mL) including sediments was also filtered and called as the sink samples for further analysis. It should also be mentioned that both hydrocyclone and DGM methods were carried out in triplicate at optimum experimental conditions in terms of the highest recovery of precious metals to ensure the results' reliability.

Table 2
Comparison of approaches about WPCBs recycling.

Methods	Feed	Aims and approaches	Results	References
Pyrometallurgy	PCBs approximately 2−3 cm^2, and 100 μm.	- To produce metal alloys by two stage heat treatments. Cu, Pb, Sn and Sb recovery at different temperatures and using different heat treatment times (400−500 °C, and 1000−1200 °C). - (PCBs exposed at 400−1350 °C, 15−60 min. - High voltage pulse generator was applied to recover copper foils at 2 KWh/kg. - Roasted (800 °C, 5 h) and further smelting (1500 °C, 2 h). PCBs were heated in vacuum pyrolysis at 500−700 °C.	- High Cu recovery (up to 94%). - Plastics and ceramics can be separated below 400 °C. - High environmental effects by evolution of toxic gases (methane, carbon monoxide, carbon dioxide, and dioxins-furans with massive carbonaceous slag formation). - Low economic benefits. - The final big metallic droplets need more leaching solutions and time to be recovered. - High energy consumptions on heating procedure.	(Hossain et al., 2018; Ulman et al., 2018a, 2018b; Shokri et al., 2017)
Physical process (floatation and multi-gravity separation methods)	PCBs powders <1.5 mm.	- Energy-intensive milling (10 h) proceed to cryo milling to produce nanoscale alloys. - Tabling, eddy current separator, floatation, multi gravity separator, and heavy media separation were used for metals recovery. - Complex triboelectric separator and air fluidization setup (0.03−15 m/s and 40 −80 m^3/h)	- Complicated steps and cost-effective equipment such as electrostatic separator, tribo-electric. separator, and cryo milling is used. - High reagent costs. - Low economic benefits. - The final metal powder was 56−72% Cu, 1−3% Fe, 7−10% Sn, and 5−8% Pb.	(Duan et al., 2009; Estrada-Ruiz et al., 2016; Guo et al., 2011; Han et al., 2016; Nekouei et al., 2018; Zhang et al., 2018a, 2018b)
Physical process (floatation and multi-gravity separation methods)	PCBs powders <0.5 mm.	- Multiple steps such as hydrocyclone, tabling, eddy current separator, floatation, and multi gravity separator are used for metals recovery.	- Coarser particles were considered for the separation. - Hydrocyclone was used only to remove the fine particles as the least metal fraction. - More complicated steps and cost-effective equipment such as eddy current separator, multi gravity separator was used. - No precious metals characterization was reported.	Das et al. (2009)
Physical process (fluidization and thermal exposure)	random access memory (RAM) cards with 100 −500 μm sieve.	- Recovery of copper values from discarded RAM cards. - Compressed air and tap water are applied and used for fluidization with airflow of 1−5 m/s. - thermal exposure of underflow at 1000 °C for 1 h is applied to achieve higher purification.	- Regarding the ICP results, Cu and Au concentrations were increased by 2 and 1.2 times, respectively (after fluidization). - 95% of metals were separated from non-metals after separation. - High energy consumptions on heating procedure was introduced. - No fine particles were considered for the separation.	Barnwal et al. (2020)
Hydrocyclone and cylindrical cyclone	plastic prills 2.8−8.0 mm	- The effect of particle flakiness on the quality of plastic particle waste density separations. - Pulp density is less than 10%, pressure 0.14 bar (hydrocyclone) and 0.40 bar (cylindrical cyclone) - Cone angel: 24°; diameter ratio (Do/Du): 27/13; total length of hydrocyclone: 303 mm and cylindrical cyclone: 420 mm.	- Separation efficiency of plastic is from 52.1% (hydrocyclone) to 100% (cylindrical cyclone). - The cylindrical design of hydrocyclone was used for increasing of separation efficiency of waste plastic particles. - No metal and fine particles were considered for the separation. - A narrow range of particle densities was selected (0.924−1.303 g/cm^3) - High-dense particle separation was not reported.	Gent et al. (2018)
Present study (Hydrocyclone and Dilution-gravity methods)	PCBs <75 μm	- The separation of valuable metals and the non-metal fraction was focused. - The e-waste volume reduction and precious metals separation at the liberation step was considered. - The hydrocyclone (3 bar), and the DGM (500 rpm, 22 °C for 5 min) allowed to achieve highest purification. - The method requires simple design.	- The total separation efficiency of Au, Pd, and Cu was obtained 75%, 78%, and 72%, respectively. - The Au, Pd, and Cu amounts are increased 2, 2.2, 3 times. - The e-waste volume reduced to 61 wt.% of the whole initial feed at the liberation step. - The sieving step separated most of the gold (73 wt.%), and palladium (66 wt.%) fractions in the finest fraction (<75 μm), while most of the copper (70 wt.%) was separated to the coarser fraction (>75 μm). - The inefficient separation of finer particles was eradicated by hydrocyclone with the separation of high dense, uniform contents. - An efficient pollution-controlled separation procedure was introduced. The water can be reused after each run. - About 87 wt.% of metals are recovered in the separated content. - Higher economic benefits. (Only water in low pressures are used, and the final fine metallic powders need lower amount of leaching solutions and time to be recovered.). It has high reliability and uses low maintenance equipment.	Present study

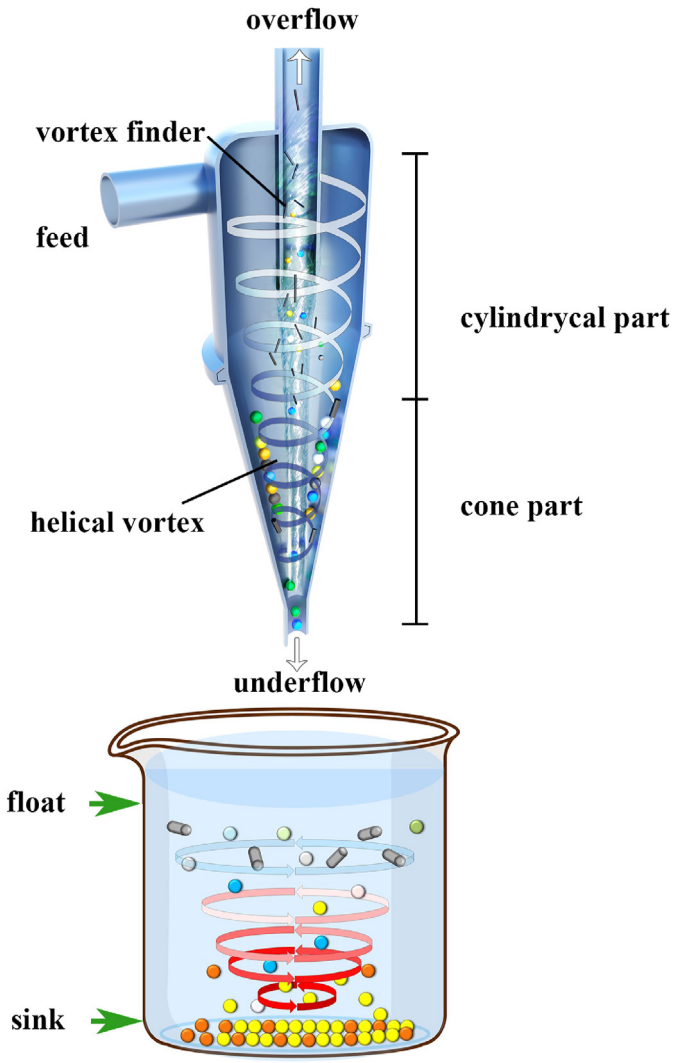

Fig. 1. Schematic of a hydrocyclone and DGM.

2.2. Characterization technique

The feed, underflow, overflow, float, and sink samples' fractions were dried at 80 °C to measure the separation efficiency and elemental concentrations. A microwave-assisted digestion technique using the SRC system (UltraWave™, Milestone, Sorisole, Italy) was utilized to dissolve 1 g of sample. The samples were weighed and added to microwave digestion vessels which were then filled with 3 mL HCl and 1 mL HNO_3 analytical grade solutions, according to the ISO standard 11,466. The vessels were sealed and pressurized with 40 bar of argon 99.999%, and then temperature and pressure were increased to 250 °C and 200 bar, respectively. After the cooling period, the samples were transferred from each tube to a new 50 mL tube and subsequently diluted using distilled water until 50 mL. Prior to each elemental analysis, the samples were initially filtered through a Phenex 0.45 mm nylon membrane syringe filter (Phenomenex Inc, US) to remove undissolved particles from the solutions. Inductively coupled plasma-mass spectrometry (ICP-MS, Agilent Technologies 7900, US) was utilized for measuring metal concentration. In addition, atomic absorption spectroscopy (AAS) (3300 AAS, Thermo Fischer Scientific, US) was more specifically used for gold concentration measurement. Furthermore, the different sizes and shapes of the particles from the initial feed, overflow, and sink samples of optimum condition were evaluated by scanning electron microscope (SEM) (Hitachi SU 3500, Japan). Energy-dispersive x-ray spectroscopy (EDS) mapping of the samples was also performed using Hitachi SU 3500 scanning electron microscope to observe elemental distributions with a carbon tape background. The software ImageJ was used to determine the length of the particles observed in SEM images. Moreover, the cumulative volume particle size distribution (PSD) of the solids in the underflow, float, and sink samples was studied by Mastersizer 3000 particle size analyzer (Malvern Co, UK).

2.3. Theory

To utilize the solid-liquid separation process to remove the non-metal fraction (NMF) and to separate the precious metal content effectively, the separation efficiencies of metals such as Au, Ag, Pd, and Cu, were calculated by the following equations (Eq. (1) and Eq. (2)) (Golmaei M. et al., 2018).

$$E_H\% = \left(\frac{m_u}{m_i}\right) \times 100, \quad (1)$$

$$E_{DGM}\% = \left(\frac{m_s}{m_u}\right) \times 100, \quad (2)$$

where m_u is the solid mass fraction of underflow and m_i is the total solid mass fraction of the underflow and overflow. m_s is the solid mass fraction of sink. All mass values are considered in grams.

The total separation efficiency (E_t) of the valuable metals can be calculated by Eq. (3) (Golmaei M. et al., 2018):

$$E_t\% = \left(\frac{m_u}{m_i}\right)\left(\frac{m_s}{m_u}\right) \times 100. \quad (3)$$

The total separation efficiency is a key parameter for the

Table 3
Hydrocyclone experiment plan.

	Sample code	Underflow diameter (mm)	Overflow to underflow diameter ratio (Do/Du)	Hydrocyclone pressure (bar)
Test 1	UF5P1	5	2.86	1
Test 2	UF5P1.5	5	2.86	1.5
Test 3	UF5P2	5	2.86	2
Test 4	UF3P1	3	4.77	1
Test 5	UF3P1.5	3	4.77	1.5
Test 6	UF3P2	3	4.77	2
Test 7	UF3P3	3	4.77	3
Test 8	UF1.5P3	1.5	9.53	3
Test 9	UF2.2P3	2.2	6.50	3

valuable metals' separation process, which gives us a viewpoint toward the total performance of both hydrocyclone and DGM methods.

The Rosin-Rammler-Bennett (RRB) model (Rosin P. A. U. L, 1933) fitting was in accordance with the size distribution model of the empirical dataset characteristics. The RRB model function calculates the spread parameter (PSD width) of the distribution (n_R) and the parameter affecting the mean size of distribution (X_R (μm)) at the different separation stage. n_R demonstrates the sharpness of separation and the particle uniformity. Therefore, it is called as the "uniformity constant". The uniformity constant n_R is the slope of ln [l/(1 - F(x)] versus x. X_R is the particle size corresponding to 63.2% (1 − l/e = 0.632) cumulative mass distribution undersize (Vesilind P. A, 1980).

The general cumulative volume form of RRB model is expressed by Eq. (4) (Rosin P. A. U. L, 1933):

$$F(x) = 1 - exp\left[-\left(\frac{X}{X_R}\right)\right]^{n_R}, \quad (4)$$

where the F(x) is the undersize distribution assuming the constant mass volume of all particles smaller than or equal to X, which is the particle size (μm). The solver tool available in Microsoft Excel software was applied to find the values of X_R and n_R. The non-linear optimization method was utilized by minimizing the residual sum of squares (RSSs). All particle size distribution data were measured twice. The average data obtained from each sample was evaluated from two different experimental results.

3. Results and discussion

3.1. Particle size, shape, and liberation characteristics

WPCBs are a multi-component system that plays essential role in both the milling and crushing steps, ultimately leading to the acquisition of different classifications for each material. Fig. 2, depicts the distribution function of the metals' size range in the WPCBs. The analysis of metals concentration in the sieved WPCBs indicates that the elemental composition varies widely in the different particle size fractions. Indeed, among the finest particles smaller than 75 μm in Fig. 2, higher gold concentration (124 mg/kg) was achieved. Therefore, higher gold concentration can be obtained by a simple sieving step. Besides, the finer fraction contained 61 wt.% of the whole e-waste. Interestingly, not only the highest gold fraction was reached by a simple mechanical liberation step, a higher copper concentration was observed in the coarser particles (200–250 μm). Meanwhile, the finest particle fraction showed the

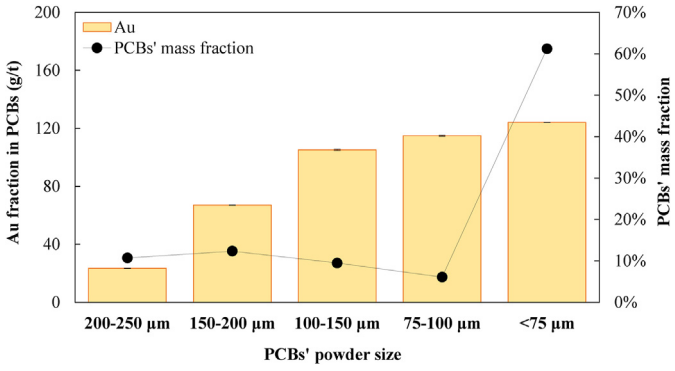

Fig. 2. Distribution of Au and PCBs' fraction in the different sieve sizes.

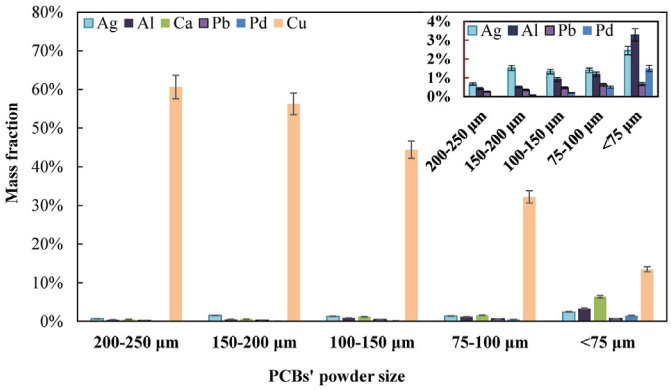

Fig. 3. Distribution of Cu, Pd, Ag, Al, Ca, and Pb fraction in the different sieve sizes.

lowest copper content. A similar trend of mass fraction distribution of WPCB over the range of less than 300 μm was observed when a two steps physical separation method to crashed WPCB was investigated (Guo C, et al., 2011; Dias P.R. et al., 2016; Barnwal A. and Dhawan N, 2020).

Fig. 3 represents the classification of metals into the different size categories after sieving. The mass fraction which was illustrated in Fig. 3, represents the Cu weight percentages among the whole considered part, including both metals and non-metals fractions. Copper has a higher thickness (>35 μm) than gold (0.05–2.54 μm) in PCBs (Vianco P. T. et al., 1996) and therefore it is also the most abundant metal in WPCB. In addition, due to its high ductility characteristics, copper is accumulated in the coarser particle fraction. However, the amount of aluminum increased from 0.42 wt.% to 2.86 wt.%, and the amount of calcium from 0.50 wt.% to 6.04 wt.% from coarser (200–250 μm) to finer (<75 μm) fraction. Such kind of metal distribution could be related to the elements in the substrate of PCB. Due to the initial fibers structure of the substrate, it is easily to cut into long-shaped rods and during sieving accumulates into finer fraction. The long needle regular structure (5–350 μm), attributed to Al, Si and Ca based on the EDS mapping results, was found for the non-metal fraction (Fig. 4b and 4.d). The diameter of these long-shaped needles was approximately 10 μm which increased their chance to pass the 75 μm sieve and end up into the finer fraction. As can be seen from Figs. 2 and 3 (ICP results) and AAS results, in feed sample (<75 μm) the metal content compared to non-metal content was lower, which might have decreased the tapped density of particles in this fraction (Barnwal A. and Dhawan N, 2020). The observed irregular shape of Au containing particles with different sizes might be ascribed to the crushing of different sections of WPCB.

SEM pictures of the finest fraction (<75 μm) are depicted in Fig. 4. Most of the gold particles were found in the following three different shapes and sizes:

- the remained oval-shaped coated Au on the Cu particles (Fig. 4a)
- coarse oval-shaped Au with the narrow rod shape fibers (Fig. 4b)
- round-shaped Au (Fig. 4c)

The average size of metal particles according to SEM analysis varied from 7 to 105 μm. According to Fig. 4.d, the majority of elements are found as round-shaped metals.

3.2. Precious metals separation

The total solids suspended (TSS) fraction of the overflow varied

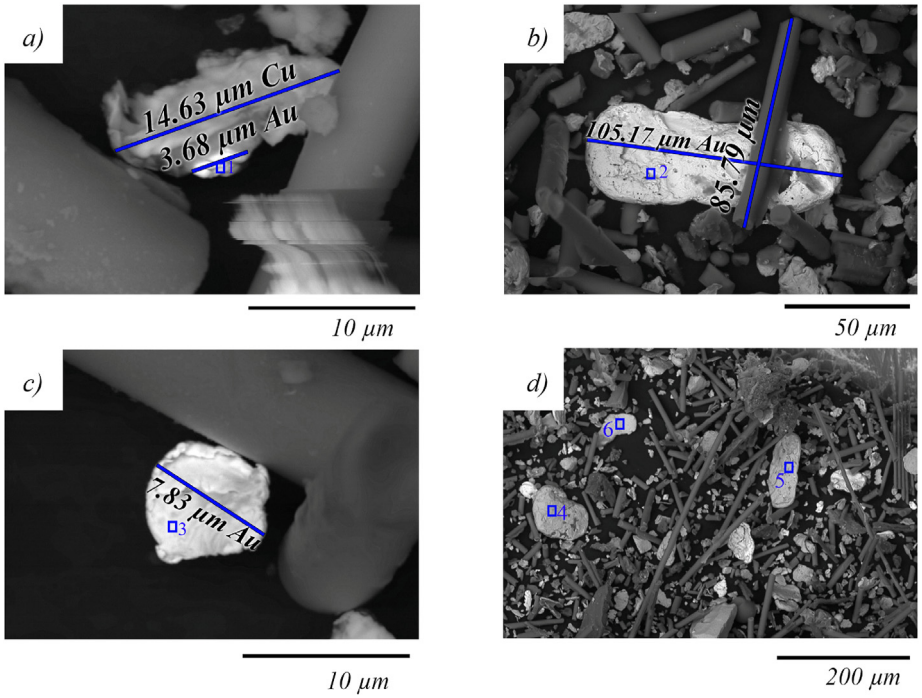

Fig. 4. SEM images of WPCBs' particles in the finest fraction (<75 μm). a) the remained coated Au on the Cu particle. b) The oval-shaped Au and the long narrow rod-shaped fibers. c) Au round shaped particle. d) The oval-shaped Cu–Sn–Pb alloy and the other round plate-shape metals (Cu, Fe, Pd, Ag, etc.). (The EDS spectrums are illustrated in the supplementary material, Fig. S1).

Table 4
TSS fraction of the underflow and sink.

Diameter ratio (Do/Du)	hydrocyclone inlet pressure (bar)	Suspended solids fraction of underflow (g)	Suspended solids fraction of sink (g)
4.77	1.0	17.61	8.89
2.86	1.0	18.71	7.74
4.77	1.5	20.17	9.59
2.86	1.5	22.62	8.10
4.77	2.0	21.81	10.49
2.86	2.0	24.68	8.90
9.53	3.0	17.98*	5.73
6.50	3.0	25.63	13.62
4.77	3.0	28.73	12.99

* Further reduction in underflow diameter will lead to loss of coarse solids to the overflow.

between 5.1 g and 8.2 g. The TSS fraction in the underflow is presented in Table 4. According to the data presented in Table 4, as the Do/Du diameter ratio increased, the TSS fraction in the underflows increased, which was also proved by (Golmaei et al., 2018). At the Do/Du diameter ratio of 9.53, an abnormal spray discharge with constant diameter known as 'rope' or 'pencil' discharge (Tian J. et al., 2020; Schneider M. and Neesse T, 2004) was replaced by the discharge in a thicker flow (Fig. 5). Due to the unusual condition of the underflow, the minimum recovery of total solids and maximum pulp density is obtained. The dilution-gravity method (DGM) was acquired by water floatation to improve high dense metals concentrations in less amount of WPCBs' powders, based on the specific gravity. Gold, palladium, silver, copper, lead, tin, and iron with high specific gravity can be separated from those with low specific gravity. When mixing started with an agitator on the upper-medium, the helical motion of the suspended solution led lighter particles to float upwards while the denser particles were concentrated in the lower central section of the vortex as sink due to gravitational forces.

Fig. 6 shows the effects of pressure and Do/Du ratio on the performance of hydrocyclone and further DGM separation for recovery of precious metals. As can be noticed, the highest separation efficiency was achieved when the experiments were accomplished at 3 bar and Do/Du ratio of 6.5. In these operating conditions, hydrocyclone followed by DGM separation could enhance the amount of gold and its total separation efficiency by 2 times and 75 wt.% compared to initial feed as can be seen in Fig. 6.a. Fig. 6.b demonstrates that the total separation efficiency of silver was 63%. At the optimum conditions, the amount of silver was increased by 22 ± 5%. The partial precipitation of Ag as AgCl in the presence of HCl (which was used to digest the samples) is inevitable, which can partially affect the accuracy of the obtained results related to the silver percentage (Fig. 6b and 3). Fig. 6.c shows, since copper is the most abundant element in the WPCBs, that the copper amount was increased up to 20 ± 4.4 wt.% by the hydrocyclone. Furthermore, the remarkable result was achieved after the second step of separation

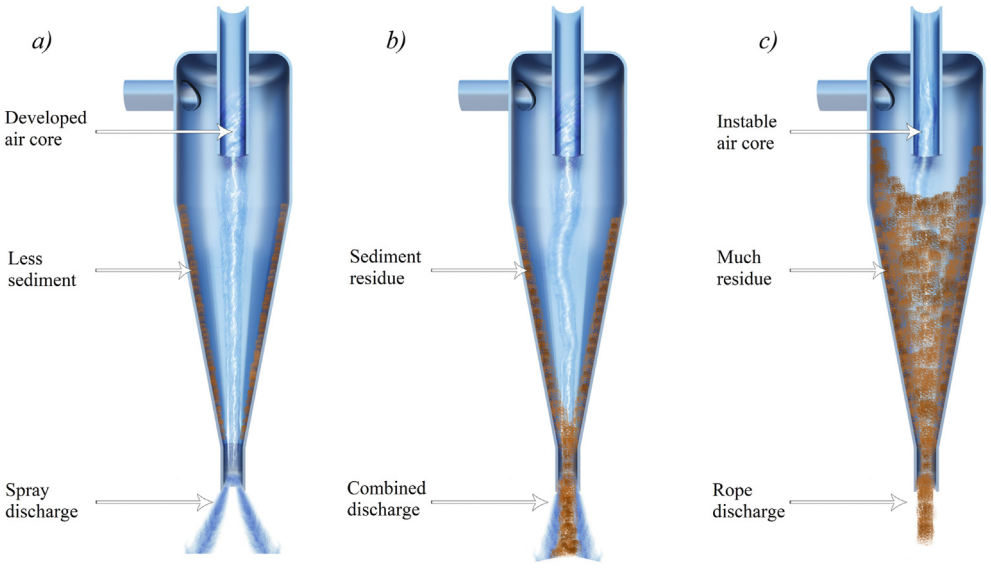

Fig. 5. The different types of discharge in the underflow of hydrocyclone, a) spray discharge b) combined discharge, and c) rope discharge.

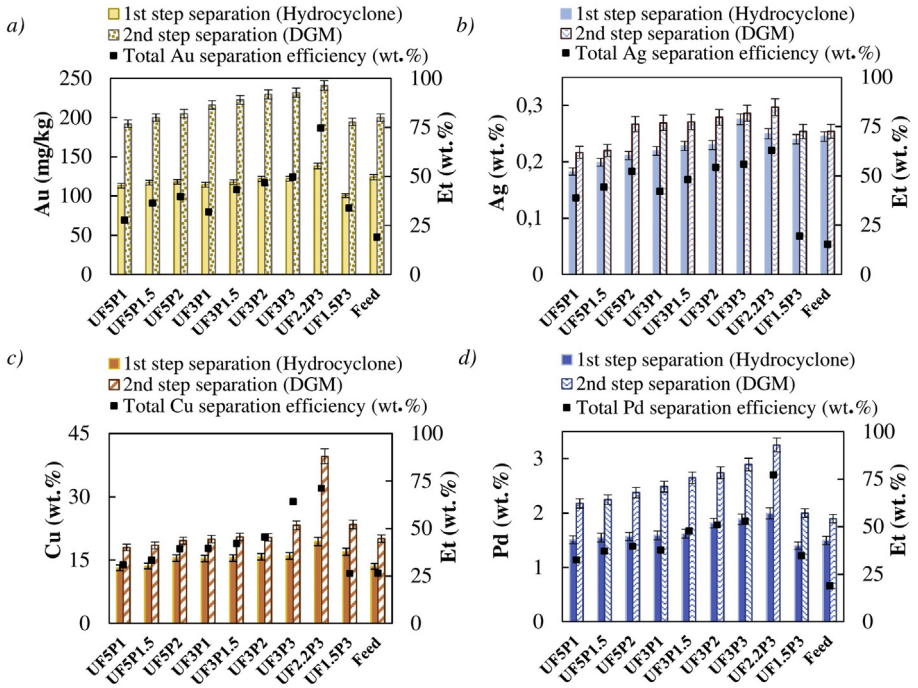

Fig. 6. Elemental analysis of the different fractions with suspended solids obtained by the 1st step (hydrocyclone) at the inlet pressures of 1, 1.5, 2, and 3 bar and the 2nd step (DGM) separation method for different metals: a) Au; b) Ag; c) Cu; d) Pd. (The standard deviations for the total efficiencies (Et) were less than 2 wt.%).

(U2.2P3 by DGM) reaching 40 ± 4 wt.% Cu (three times higher) at the end of the process with the separation efficiency of 72%. Fig. 6.d shows palladium as the second-highest dense metal fraction in the WPCBs. In addition to the successful separation step by the hydrocyclone for Pd, the second step of separation increased the percentage of Pd 2.17 times higher compared to the initial feed. Additionally, the total separation efficiency of Pd was 78%. The mass balance error was obtained between 0.08 and 1%.

In Fig. 6, the solid filled columns in the feed sample show the initial WPCBs' values. The second step separation (the pattern fill columns) in the feed columns indicates the DGM method results without a hydrocyclone separation step. According to the results, hydrocyclone and DGM method's application clearly increased the total separation efficiency and the content of precious metals in the final concentrated particles. In DGM, due to the helical motion of the suspended solution from a larger radius at the top to the smaller one at the bottom, lower flotation was observed for the high dense contents of sink samples obtained by hydrocyclone.

Table 5
The ICP results (wt.%) of the other elements for the feed, overflow, underflow, and sink samples of optimum condition at the Do/Du of 6.50 and the inlet pressure of 3 bar.

Symbol of element	Feed	overflow	1st step separation (underflow)	2nd step separation (sink)
Fe	3.88	1.57	5.02	19.1
Sn	5.18	3.98	6.02	7.42
Ni	0.41	0.33	0.5	1.61
Zn	0.82	0.91	0.97	1.27
Pb	0.66	0.57	0.72	1.07
Ca	6.82	3.16	6.06	0.59
Al	3.28	2.09	3.23	0.57
Na	0.29	0.22	0.29	0.13
Cr	0.04	0.10	0.05	0.13
Mn	0.018	0.02	0.02	0.07
Mg	0.17	0.17	0.14	0.04
Co	0.006	0.009	0.007	0.021
Sb	0.07	0.13	0.03	0.01
K	0.049	0.039	0.062	0.006
Bi	0.004	0.006	0.003	0.005
Mo	0.003	0.011	0.003	0.005

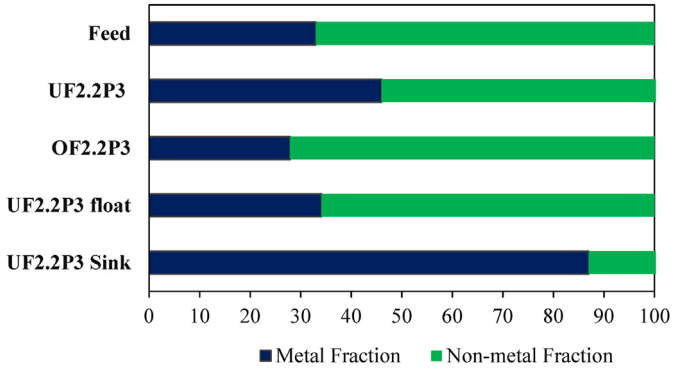

Fig. 7. The hydrocyclone (UF2.2P3 and OF2.2P3) and DGM (UF2.2P3 sink and float) method separated metals/non-metal fractions (wt.%) in the optimum condition.

From the authors' point of view, the elemental analysis results prove that the inefficient separation of finer particles can be eradicated by hydrocyclone as feasible and straightforward equipment. According to the previous studies (Barnwal A. and Dhawan N, 2020), particle size below 100 μm is unfavorable when the separation process is being utilized merely by the gravity method. However, the hydrocyclone separation method leads to attaining less agglomerated and more uniform particles for the DGM.

In Table 5, the weight percent fractions of other elements are presented. As can be seen, substantial separation improvements are found for Fe and Sn at both the first and second steps of the separation procedures. The high density, abundance, and size characteristics of iron and tin compared to the other elements of the list led to an increase in the amount of Fe and Sn in the underflow and sink. In addition, Ni, Zn, Pb, Cr, Mn, Co, Bi, and Mo were mostly collected in the sink. Contrary to the others, the high Ca, Al, Na, Mg, Sb, and K flotation was observed in the DGM method.

The applied separation procedures' desired outcome is a decrease of non-metal contents in the WPCBs' powders. As can be seen in Fig. 7, based on the sum of elemental mass values obtained from the ICP and AAS results and defining the dissolved elements, 72% of the fine non-metal components contained at the overflow fraction. On the contrary, 46% of relatively uniform metals in accordance with their shape, size, and density were mainly collected at the underflow. Furthermore, it was observed that the amount of non-metal fraction (NMF) in the initial feed was decreased from 68% to 13% in the sink sample (UF2.2P3 sink). Based on the ICP and AAS analyses, 87% of the UF2.2P3-sink fraction was dissolved as a metal fraction. According to the weighed samples before and after dissolution in the acid, 89% of the optimum condition (UF2.2P3-sink) sample was dissolved. In this method, besides the metal elements, oxygen and silicon could be considered as the missing elements in the separated fractions' compositions.

The PSD of solids in the underflow, float, sink, and the initial feed samples are illustrated in Fig. 8. The effects of the overflow to underflow outlet diameter ratio (Do/Du) on the particle size distributions for each fraction are depicted. Furthermore, the experimental particle size distribution results are assigned to the Rosin-Rammler-Bennett model for each sample, and the RRB model parameters are assigned to the legend of Fig. 8.

The large distribution of the separated solids with the hydrocyclone and DMG methods was acquired in Fig. 8. Regarding the representative evaluation of particle size distribution and achieved mean particle size parameters (X_R), mainly the finer and less dense particles were migrated to the overflow, whereas the coarser particles were collected in the underflow and especially sink. Based on the results, significant separation of finer particles was improved by increasing the overflow to underflow outlet diameter ratio (Do/Du) and inlet pressures. The smaller underflow diameter and higher inlet pressure led to obtaining coarser particles in the underflow, which was confirmed also by (Golmaei et al., 2018; Cilliers J. J, 2000; Hwang et al., 2008, and Frachon and Cilliers, 1999). Furthermore, these results are in accordance with the elemental values measured by the ICP and AAS analysis.

At the DMG step, further fluidization of finer particles was achieved at the float samples. According to Fig. 8.a, the float fraction at the Do/Du parameter of 4.77, finer particles were observed compared to the float fraction of the Do/Du parameter of 2.86 at the inlet pressure of 2 bar. In addition, the finest float fraction at Do/Du parameter of 6.5 at an inlet pressure of 3 bar was attained due to the efficient separation of solids in the underflow fraction, which led to the coarser and denser suspension in the sink fraction. In other words, at the higher separation efficiency, the finer and lighter particles were migrated to the overflow. Therefore, the float fraction of the sample at the highest separation efficiency was obtained from a significant coarser fraction (Do/Du = 6.5 − underflow). The RRB model data presented in Fig. 8.b defines that the highest mean particle size parameters (X_R) were separated at the sink (Do/Du = 6.5 − Sink).

The SEM backscattered electron beam images of the initial feed and the separated fraction in the underflow confirmed the separation results (Fig. 9). The coarser uniform particles were collected at the end of the two-step separation procedure, which confirms

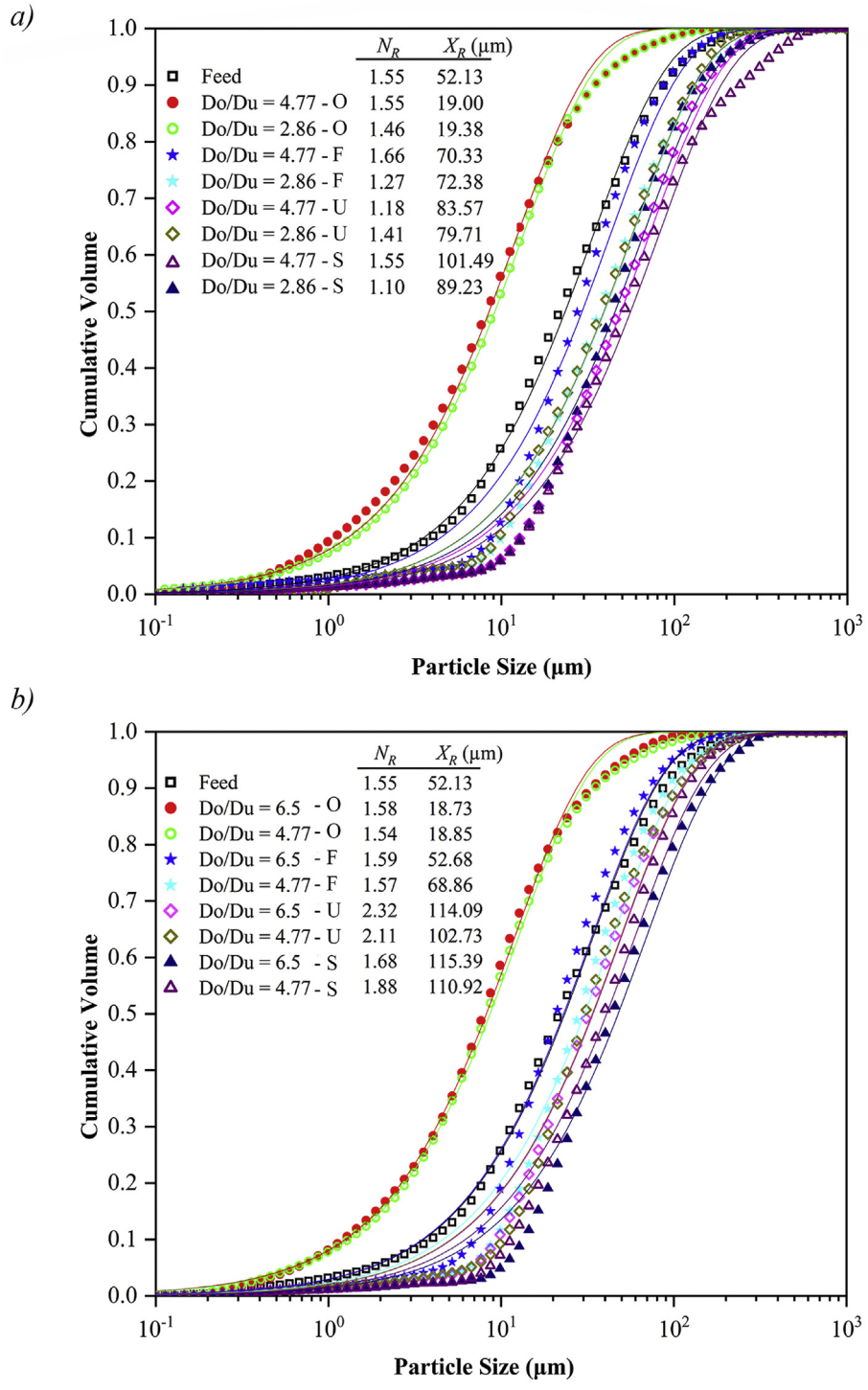

Fig. 8. The overflow to underflow outlet diameter ratio (Do/Du) empirical characteristics on the particle size distribution in the overflow, underflow, float, and sink at the inlet pressure of 2 bar (a) and 3 bar (b). The Rosin-Rammler-Bennett (RRB) fitted model is defined with line. The spread parameters of the distribution (nR) and the mean particle size parameters (XR) are presented in the legends. (O: Overflow, F: Float, U: Underflow, and S: Sink).

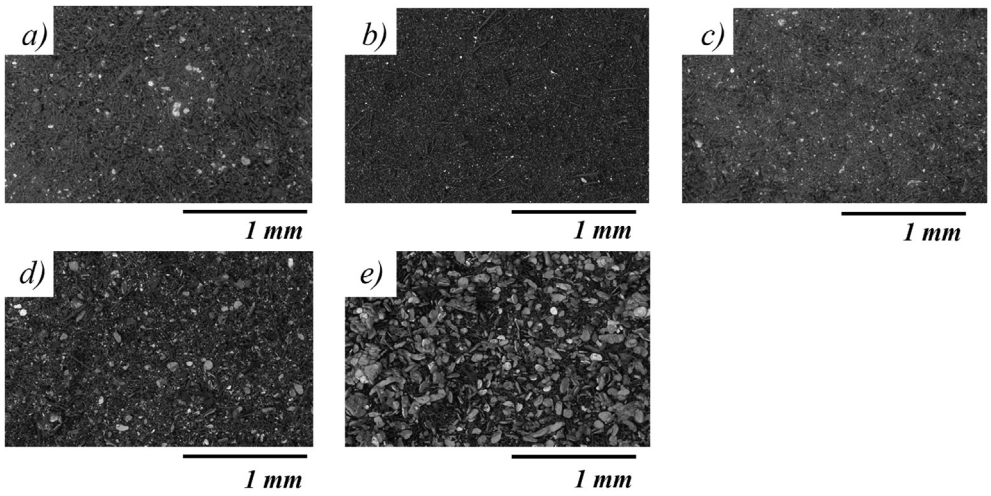

Fig. 9. SEM images of a) initial feed (<75 μm), b) the overflow fraction, c) the float fraction, d) the underflow fraction, e) sink fraction of optimum condition. Sample UF2.2P3.

particle size distribution analysis and RRB model results. As Fig. 9.b shows most of the fiber rods were separated from the overflow's initial feed. In Fig. 9.c, more fiber rods were separated within the fine metals in the float. As can be noted, no coarse particles remained within the overflow and float samples. Fig. 9.d illustrates the underflow from the hydrocyclone separation step. As a comparison to Fig. 9.a, fewer fiber rods and more round plate-shaped particles were observed in Fig. 9.d. Further, in Fig. 9.e, coarser grains were divided from the underflow sample in the second step of the separation (DMG). Since more fiber rods were separated in the float fraction, fewer fiber rods can be seen in the sink sample. These results are in parallel with the RRB model and particle size distribution experimental results in Fig. 9.

EDS maps were acquired from the initial feed and the optimum separated sample (UF2.2P3 – Sink). According to Fig. 10, precious metals are distributed homogeneously in the samples. Fig. 10a and 10.b illustrate that Ca, Al, and Si are the fiber rods' main components. The Cu, Fe, Sn, Pb, and Ag elemental phase distribution in the optimum separated sample (UF2.2P3 – Sink) confirms the separation of coarser grains at the end of the process which was indicated in the particle size distribution analysis. Finally, in order to obtain a better understanding of the subject, the selected processes for the efficient separation of valuable metals are addressed with a simplified flowchart represented in Fig. 11.

4. Conclusions

Efficient separation of precious metals from WPCBs to highly concentrated content can lead to industrial prospects in urban mining. In this study, a sustainable, green, and simple method was utilized to investigate different particles' separation behavior based on their size, shape, and density. At the preliminary stage, the different liberation characteristics of metals and non-metals in the grinding step led to the separation of 61 wt.% of the e-waste mass volume in the finest fraction (<75 μm). Interestingly, most of the gold (73 wt.%), palladium (66 wt.%), and silver (33 wt.%) were acquired in the finest fraction (<75 μm), while most of the copper (70 wt.%) was separated to the coarser fraction (>75 μm) by a simple grinding. Although the separation efficiency of the fine powders (<100 μm) are considered more challenging due to the higher amount of non-metal fractions (NMF) and fibers, the hydrocyclone technique was shown as a valuable method for the separation of high dense, uniform content from the initial feed. In the first step, the effects of the hydrocyclone variables in the separated precious metals were studied. The overflow fraction contained 72% of the fine non-metal fractions separated. On the contrary, the content with 46% of moderately uniform metals was collected mainly at the underflow. The results showed that the higher overflow to underflow outlet diameter (Do/Du = 6.5) and higher inlet pressure (3 bar) of the hydrocyclone positively impacted on the separation of precious metals to the underflow, and 87 wt.% separation of metal fractions into the sink. Moreover, the dilution-gravity method (DGM), as a second step, enhanced the final collected metal fraction. The total separation efficiency of gold, palladium, silver, and copper was obtained 75%, 78%, 64%, and 72%, respectively.

CRediT authorship contribution statement

Mohammad Reza Bilesan: Investigation, Writing - original draft, Writing - review & editing, Formal analysis, Software, Conceptualization, Methodology. **Irina Makarova:** Investigation, Writing - review & editing, Conceptualization, Formal analysis. **Björn Wickman:** Supervision, Writing - review & editing, Conceptualization. **Eveliina Repo:** Supervision, Project administration, Funding acquisition, Writing - review & editing, Conceptualization.

Declaration of competing interest

The authors declare that they have no known competing financial interests or personal relationships that could have appeared to influence the work reported in this paper.

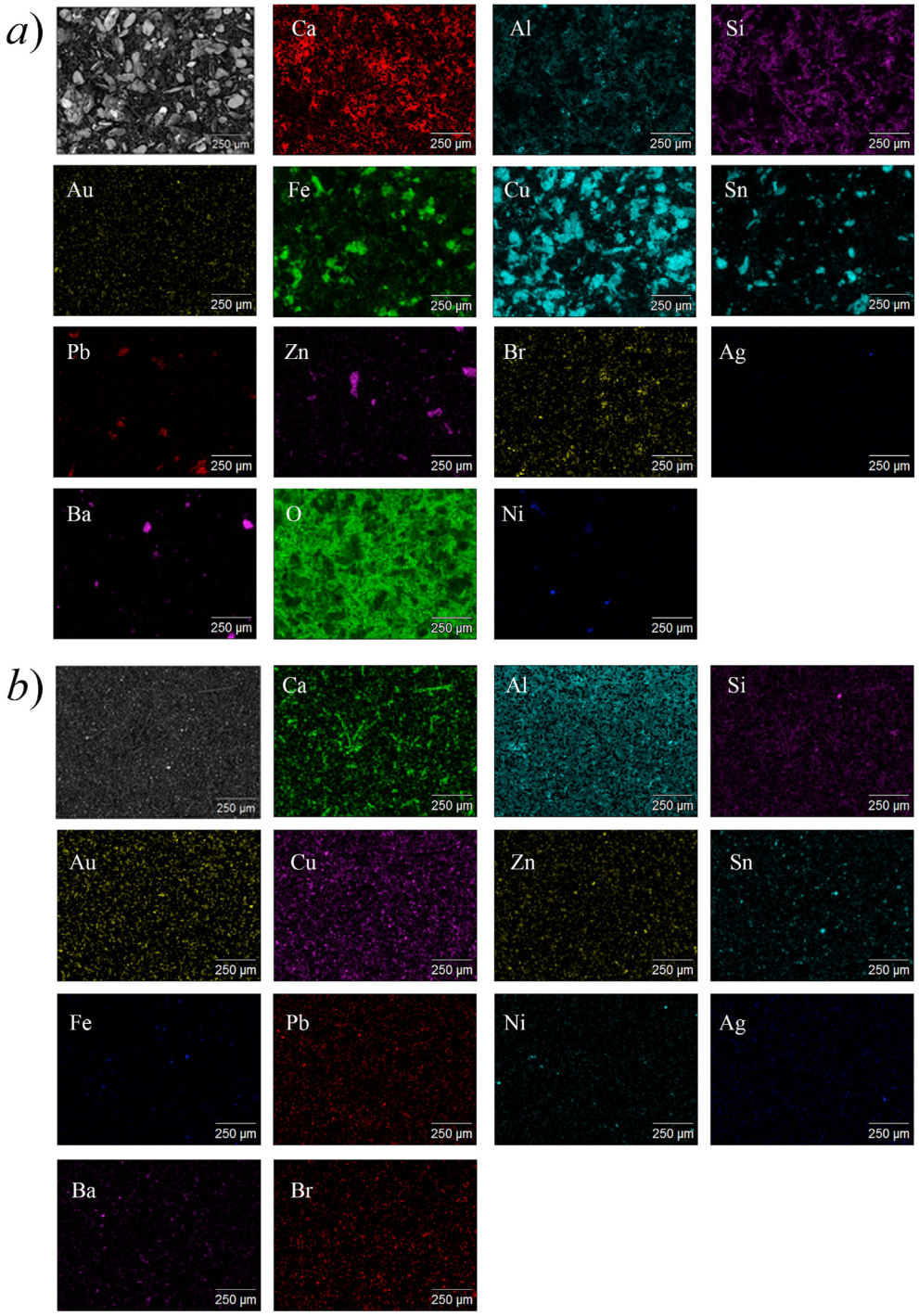

Fig. 10. SEM-EDS elemental mapping in the optimum condition, a) underflow sample UF2.2P3; b) overflow OF2.2P3.

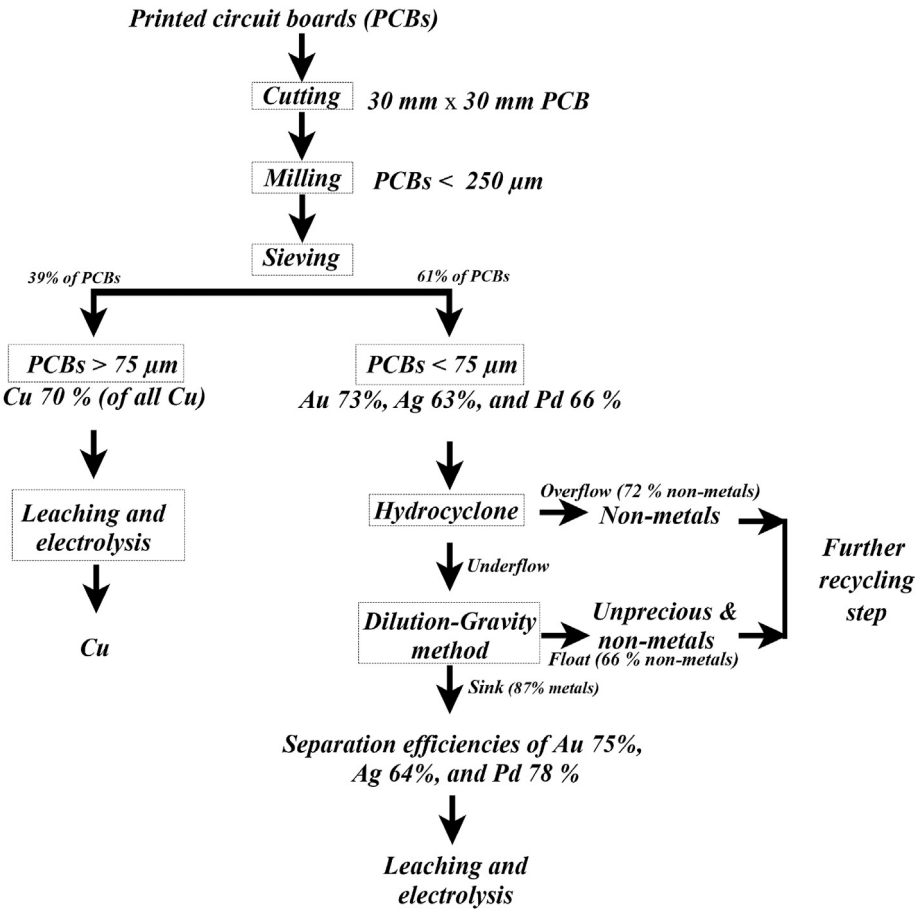

Fig. 11. Flowchart of the valuable metals' recovery from PCBs by hydrocyclone and DGM.

Acknowledgements

This study was supported by Academy of Finland (Grant No. 325002). The authors would like to acknowledge Mohammadamin Esmaeili for his precious comments and help in revising of the manuscript, Liisa Puro, and Toni Väkiparta for their helpful suggestions and guidance with ICP and SEM measurements.

Appendix A. Supplementary data

Supplementary data to this article can be found online at https://doi.org/10.1016/j.jclepro.2020.125505.

References

Bai, Z.S., Wang, H.L., Tu, S.T., 2009. Removal of catalyst particles from oil slurry by hydrocyclone. Separ. Sci. Technol. 44 (9), 2067–2077. https://doi.org/10.1080/01496390902880149.

Barnwal, A., Dhawan, N., 2020. Recovery of copper values from discarded random access memory cards via fluidization and thermal exposure. J. Clean. Prod. 256, 120516. https://doi.org/10.1016/j.jclepro.2020.120516.

Barnwal, A., Dhawan, N., 2020. Recycling of discarded mobile printed circuit boards for extraction of gold and copper. Sustainable Materials and Technologies. p.e00164. https://doi.org/10.1016/j.susmat.2020.e00164.

Behnamfard, A., Salarirad, M.M., Veglio, F., 2013. Process development for recovery of copper and precious metals from waste printed circuit boards with emphasize on palladium and gold leaching and precipitation. Waste Manag. 33 (11), 2354–2363. https://doi.org/10.1016/j.wasman.2013.07.017.

Bleiwas, D., Kelly, T., 2001. Obsolete computers, "Gold mines," or high-tech trach? Resource recovery from recycling[R], United States geological survey, 7. https://doi.org/10.3133/fs06001.

Birloaga, I., De Michelis, I., Ferella, F., Buzatu, M., Vegliò, F., 2013. Study on the influence of various factors in the hydrometallurgical processing of waste printed circuit boards for copper and gold recovery. Waste Manag. 33 (4), 935–941. https://doi.org/10.1016/j.wasman.2013.01.003.

Bizzo, W.A., Figueiredo, R.A., De Andrade, V.F., 2014. Characterization of printed circuit boards for metal and energy recovery after milling and mechanical separation. Materials 7 (6), 4555–4566. https://doi.org/10.3390/ma7064555.

Cilliers, J.J., 2000. Hydrocyclones for particle size separation. Part. Size Sepp. 1819–1825. https://doi.org/10.1016/B0-12-226770-2/06881-2.

Cui, J., Forssberg, E., 2003. Mechanical recycling of waste electric and electronic equipment: a review. J. Hazard Mater. 99 (3), 243–263. https://doi.org/10.1016/S0304-3894(03)00061-X.

Cui, J., Zhang, L., 2008. Metallurgical recovery of metals from electronic waste: a review. J. Hazard Mater. 158 (2–3), 228–256. https://doi.org/10.1016/j.jhazmat.2008.02.001.

Cullivan, J.C., Williams, R.A., Dyakowski, T., Cross, C.R., 2004. New understanding of a hydrocyclone flow field and separation mechanism from computational fluid dynamics. Miner. Eng. 17 (5), 651–660. https://doi.org/10.1016/j.mineng.2004.04.009.

Das, A., Vidyadhar, A., Mehrotra, S.P., 2009. A novel flowsheet for the recovery of metal values from waste printed circuit boards. Resour. Conserv. Recycl. 53 (8), 464–469. https://doi.org/10.1016/j.resconrec.2009.03.008.

Deveci, H., Yazıcı, E.Y., Aydın, U., Yazıcı, R., Akcil, A., 2010. Extraction of copper from scrap TV boards by sulphuric acid leaching under oxidising conditions. In: Proceedings of Going Green-CARE INNOVATION 2010 Conference, p. 45, 8–11 November, Vienna, Austria.

Dias, P.R., Benevit, M.G., Veit, H.M., 2016. Photovoltaic solar panels of crystalline silicon: characterization and separation. Waste Manag. Res. 34 (3), 235–245. https://doi.org/10.1177/0734242X15622812.

Duan, C., Wen, X., Shi, C., Zhao, Y., Wen, B., He, Y., 2009. Recovery of metals from waste printed circuit boards by a mechanical method using a water medium. J. Hazard Mater. 166 (1), 478–482. https://doi.org/10.1016/j.jhazmat.2008.11.060.

Estrada-Ruiz, R.H., Flores-Campos, R., Gámez-Altamirano, H.A., Velarde-Sánchez, E.J., 2016. Separation of the metallic and non-metallic fraction from printed circuit boards employing green technology. J. Hazard Mater. 311, 91–99. https://doi.org/10.1016/j.jhazmat.2016.02.061.

Fogarasi, S., Imre-Lucaci, F., Imre-Lucaci, Á., Ilea, P., 2014. Copper recovery and gold enrichment from waste printed circuit boards by mediated electrochemical

oxidation. J. Hazard Mater. 273, 215–221. https://doi.org/10.1016/j.jhazmat.2014.03.043.
Frachon, M., Cilliers, J., 1999. A general model for hydrocyclone partition curves. Chem. Eng. J. 73, 53–59. https://doi.org/10.1016/S1385-8947(99)00040-6.
Fu, S., Hua, W., Yuan, H., Ling, J., Shi, Q., 2019. Study on the light medium separation of waste plastics with hydrocyclones. Waste Manag. 91, 54–61. https://doi.org/10.1016/j.wasman.2019.04.043.
Fujita, T., Ono, H., Dodbiba, G., Yamaguchi, K., 2014. Evaluation of a recycling process for printed circuit board by physical separation and heat treatment. Waste Manag. 34 (7), 1264–1273. https://doi.org/10.1016/j.wasman.2014.03.002.
Gent, M., Sierra, H.M., Álvarez, M.M., McCulloch, J., 2018. An evaluation of hydrocyclones and the LARCODEMS cylindrical cyclone for the separation of waste plastics of proximate densities. Waste Manag. 79, 374–384. https://doi.org/10.1016/j.wasman.2018.08.004.
Ghadirian, M., Afacan, A., Hayes, R.E., Mmbaga, J.P., Mahmood, T., Xu, Z., Masliyah, J., 2015. A study of the hydrocyclone for the separation of light and heavy particles in aqueous slurry. Can. J. Chem. Eng. 93 (9), 1667–1677. https://doi.org/10.1002/cjce.22252.
Golmaei, M., Kinnarinen, T., Jernström, E., Häkkinen, A., 2018. Efficient separation of hazardous trace metals and improvement of the filtration properties of green liquor dregs by a hydrocyclone. J. Clean. Prod. 183, 162–171. https://doi.org/10.1016/j.jclepro.2018.02.123.
Gonçalves, S.M., Barrozo, M.A., Vieira, L.G., 2017. Effects of solids concentration and underflow diameter on the performance of a newly designed hydrocyclone. Chem. Eng. Technol. 40 (10), 1750–1757. https://doi.org/10.1002/ceat.201600496.
Goodship, V., Stevels, A., Huisman, J. (Eds.), 2019. Waste Electrical and Electronic Equipment (WEEE) Handbook. Woodhead Publishing.
Gramatyka, P., Nowosielski, R., Sakiewicz, P., 2007. Recycling of waste electrical and electronic equipment. J. Achiev. Mater. Manuf. Eng. 20 (1–2), 535–538. https://www.researchgate.net/publication/42253354_Recycling_of_waste_electrical_and_electronic_equipment.
Gray, T., 2012. Elements: A Visual Exploration of Every Known Atom in the Universe. Black Dog & Leventhal Publishing, Inc, Hachette UK.
Guarnieri, P., e Silva, L.C., Xavier, L.H., Chaves, G.L.D., 2020. Recycling challenges for electronic consumer products to E-waste: a developing countries' perspective. In: E-waste Recycling and Management. Springer, Cham, pp. 81–110.
Guo, J., Guo, J., Xu, Z., 2009. Recycling of non-metallic fractions from waste printed circuit boards: a review. J. Hazard Mater. 168 (2–3), 567–590. https://doi.org/10.1016/j.jhazmat.2009.02.104.
Guo, C., Wang, H., Liang, W., Fu, J., Yi, X., 2011. Liberation characteristic and physical separation of printed circuit board (PCB). Waste Manag. 31 (9–10), 2161–2166. https://doi.org/10.1016/j.wasman.2011.05.011.
Han, Y., He, W., Li, L., Li, G., Huang, J., 2016. Mathematical analysis of the gas–solid fluidized bed separation of metals and nonmetals from waste PCB powders. Powder Technol. 295, 142–151. https://doi.org/10.1016/j.powtec.2016.03.040.
He, W., Li, G., Ma, X., Wang, H., Huang, J., Xu, M., Huang, C., 2006. WEEE recovery strategies and the WEEE treatment status in China. J. Hazard Mater. 136 (3), 502–512. https://doi.org/10.1016/j.jhazmat.2006.04.060.
Hino, T., Agawa, R., Moriya, Y., Nishida, M., Tsugita, Y., Araki, T., 2009. Techniques to separate metal from waste printed circuit boards from discarded personal computers. J. Mater. Cycles Waste Manag. 11, 42–54. https://doi.org/10.1007/s10163-008-0218-0.
Hossain, R., Nekouei, R.K., Mansuri, I., Sahajwalla, V., 2018. Sustainable recovery of Cu and Sn from problematic global waste: exploring value from waste printed circuit boards. ACS Sustain. Chem. Eng. 7 (1), 1006–1017. https://doi.org/10.1021/acssuschemeng.8b04657.
Huisman, J., 2012. Eco-efficiency evaluation of WEEE take-back systems. In: Waste Electrical and Electronic Equipment (WEEE) Handbook. Woodhead Publishing, pp. 93–119. https://doi.org/10.1533/9780857096333.1.93.
Hwang, K.J., Wu, W.H., Qian*, S., Nagase, Y., 2008. CFD study on the effect of hydrocyclone structure on the separation efficiency of fine particles. Separ. Sci. Technol. 43 (15), 3777–3797. https://doi.org/10.1080/01496390802286637.
Ilyas, S., Lee, J.C., Kim, B.S., 2014. Bioremoval of heavy metals from recycling industry electronic waste by a consortium of moderate thermophiles: process development and optimization. J. Clean. Prod. 70, 194–202. https://doi.org/10.1016/j.jclepro.2014.02.019.
Kumar, A., Holuszko, M., Janke, T., 2018. Separating inorganics from the non-metal fraction of the processed waste PCBS using heavy liquid separation. Int J Waste Resour 8 (355), 2. https://doi.org/10.1016/j.wasman.2018.02.010.
Le, H.L., Yamasue, E., Okumura, H., Ishihara, K.N., 2014. Improving sustainable recovery of metals from waste printed circuit boards by the primary copper smelter process. J. Mater. Cycles Waste Manag. 16 (2), 298–305. https://doi.org/10.1007/s10163-013-0189-7.
Lee, J.C., Srivastava, R.R., 2016. Leaching of Gold from the Spent/end-Of-Life Mobile Phone-PCBs Using "Greener Reagents". The Recovery of Gold from Secondary Sources, vols. 7–56. Imperial College Press.
Lehner, T., 1998. Integrated recycling of non-ferrousmetal at boliden ltd. In: Proceedings of the IEEE International Symposium on Electronics and the Environment, pp. 42–47. https://doi.org/10.1109/ISEE.1998.675028, 1998.
Murthy, Y.R., Tripathy, S.K., Kumar, C.R., 2011. Chrome ore beneficiation challenges & opportunities–A review. Miner. Eng. 24 (5), 375–380. https://doi.org/10.1016/j.mineng.2010.12.001.
Nekouei, R.K., Pahlevani, F., Rajarao, R., Golmohammadzadeh, R., Sahajwalla, V., 2018. Direct transformation of waste printed circuit boards to nano-structured powders through mechanical alloying. Mater. Des. 141, 26–36. https://doi.org/10.1016/j.matdes.2017.12.032.
Nie, C.C., Wang, Y.Y., Zhang, H., Zhang, Y.K., Zhang, Y.Q., Yan, Z.Q., Li, B., Lyu, X.J., Tao, Y.J., Qiu, J., Li, L., 2020. Cleaner utilization of non-metallic components in separation tailings of waste printed circuit board: pyrolysis oil, calorific value and building aggregate. J. Clean. Prod. 120976. https://doi.org/10.1016/j.jclepro.2020.120976.
Oishi, T., Koyama, K., Alam, S., Tanaka, M., Lee, J.C., 2007. Recovery of high purity copper cathode from printed circuit boards using ammoniacal sulfate or chloride solutions. Hydrometallurgy 89 (1–2), 82–88. https://doi.org/10.1016/j.hydromet.2007.05.010.
Purchase, D., Abbasi, G., Bisschop, L., Chatterjee, D., Ekberg, C., Ermolin, M., Fedotov, P., Garelick, H., Isimekhai, K., Kandile, N.G., Lundström, M., 2020. Global occurrence, chemical properties, and ecological impacts of e-wastes (IUPAC technical report). Pure Appl. Chem. 1 https://doi.org/10.1515/pac-2019-0502 (ahead-of-print).
Ren, Y., Zhang, X., Wei, H., Xu, L., Zhang, J., Sun, J., Wang, X., Li, W., 2017. Comparisons of methods to obtain insoluble particles in snow for transmission electron microscopy. Atmos. Environ. 153, 61–69. https://doi.org/10.1016/j.atmosenv.2017.01.021.
Rosin, P.A.U.L., 1933. Laws governing the fineness of powdered coal. J. Inst. Fuel 7, 29–36.
Ruediger, K., 2011. Solving the E-Waste Problem (Step) Initiative: Annual Report. United Nations University, p. 32.
Schneider, M., Neesse, T., 2004. Overflow-control system for a hydrocyclone battery. Int. J. Miner. Process. 74, S339–S343. https://doi.org/10.1016/j.minpro.2004.07.037.
Schubert, G., 1991. Aufbereitung der NE-Metallschrotte und NE-metallhaltigen Abfälle. II. Aufbereit. - Tech. 32 (7), 352–358.
Shokri, A., Pahlevani, F., Cole, I., Sahajwalla, V., 2017. Selective thermal transformation of old computer printed circuit boards to Cu-Sn based alloy. J. Environ. Manag. 199, 7–12. https://doi.org/10.1016/j.jenvman.2017.05.028.
Svarovsky, L., 2000. Solid-liquid Separation. Elsevier.
Sun, Y., Fu, G., Jiang, L., 2018. Reductive Leaching of Low-Grade Manganese Oxide Ores Using Pretreated Straw as Reductant. Mineral Processing and Extractive Metallurgy, pp. 1–6. https://doi.org/10.1080/25726641.2018.1505210.
Tian, J., Wang, H., Lv, W., Huang, Y., Fu, P., Li, J., Liu, Y., 2020. Enhancement of pollutants hydrocyclone separation by adjusting back pressure ratio and pressure drop ratio. Separ. Purif. Technol. 240, 116604. https://doi.org/10.1016/j.seppur.2020.116604.
Tiwary, C.S., Kishore, S., Vasireddi, R., Mahapatra, D.R., Ajayan, P.M., Chattopadhyay, K., 2017. Electronic waste recycling via cryo-milling and nanoparticle beneficiation. Mater. Today 20 (2), 67–73. https://doi.org/10.1016/j.mattod.2017.01.015.
Ulman, K., Ghose, A., Maroufi, S., Mansuri, I., Sahajwalla, V., 2018. Disentanglement of random access memory cards to regenerate copper foil: a novel thermo-electrical approach. Waste Manag. 81, 138–147. https://doi.org/10.1016/j.wasman.2018.10.002.
Ulman, K., Maroufi, S., Bhattacharyya, S., Sahajwalla, V., 2018. Thermal transformation of printed circuit boards at 500° C for synthesis of a copper-based product. J. Clean. Prod. 198, 1485–1493. https://doi.org/10.1016/j.jclepro.2018.07.140.
Vasile, C., Brebu, M.A., Totolin, M., Yanik, J.A.L.E., Karayildirim, T.A.M.E.R., Darie, H., 2008. Feedstock recycling from the printed circuit boards of used computers. Energy Fuels 22 (3), 1658–1665. https://doi.org/10.1021/ef700659t.
Vesilind, P.A., 1980. The Rosin-Rammler particle size distribution. Resour. Recovery Conserv. 5 (3), 275–277. https://doi.org/10.1016/0304-3967(80)90007-4.
Vianco, P.T., 1993. Embrittlement of Surface Mount Solder Joints by Hot Solder-Dipped, Gold-Plated Leads (No. SAND-93-0082C; CONF-9308126-3). Sandia National Labs., Albuquerque, NM (United States).
Vianco, P.T., Hosking, F.M., Rejent, J.A., 1996. Ultrasonic soldering for structural and electronic applications. Welding Journal-Including Welding Research Supplement 75 (11), 343s.
Vieira, L.G., Barrozo, M.A., 2014. Effect of vortex finder diameter on the performance of a novel hydrocyclone separator. Miner. Eng. 57, 50–56. https://doi.org/10.1016/j.mineng.2013.11.014.
Xue, M., Yang, Y., Ruan, J., Xu, Z., 2012. Assessment of noise and heavy metals (Cr, Cu, Cd, Pb) in the ambience of the production line for recycling waste printed circuit boards. Environ. Sci. Technol. 46 (1), 494–499. https://doi.org/10.1021/es202513b.
Xue, M., Li, J., Xu, Z., 2013. Management strategies on the industrialization road of state-of-the-art technologies for e-waste recycling: the case study of electrostatic separation—a review. Waste Manag. Res. 31 (2), 130–140. https://doi.org/10.1177/0734242X12465464.
Yang, T., Xu, Z., Wen, J., Yang, L., 2009. Factors influencing bioleaching copper from waste printed circuit boards by Acidithiobacillus ferrooxidans. Hydrometallurgy 97 (1–2), 29–32. https://doi.org/10.1016/j.hydromet.2008.12.011.
Zhang, S., Ding, Y., Liu, B., Pan, D.A., Chang, C.C., Volinsky, A.A., 2015. Challenges in legislation, recycling system and technical system of waste electrical and electronic equipment in China. Waste Manag. 45, 361–373. https://doi.org/10.1016/j.wasman.2015.05.015.
Zhang, G., He, Y., Feng, Y., Zhang, T., Wang, H., Zhu, X., 2018a. Recovery of residual metals from fine nonmetallic fractions of waste printed circuit boards using a vibrated gas-solid fluidized bed. Separ. Purif. Technol. 207, 321–328.
Zhang, G., Wang, H., Yang, J., He, Y., Zhang, T., 2018b. Application of electric field to a

fluidized bed for recovering residual metals from fine particles of the non-metallic fraction of waste printed circuit boards. J. Clean. Prod. 187, 1036–1042. https://doi.org/10.1016/j.jclepro.2018.03.282.
Zhou, L., Xu, Z., 2012. Response to waste electrical and electronic equipments in China: legislation, recycling system, and advanced integrated process. Environ. Sci. Technol. 46 (9), 4713–4724. https://doi.org/10.1021/es203771m.
Zhu, X.N., Nie, C.C., Wang, S.S., Xie, Y., Zhang, H., Lyu, X.J., Qiu, J., Li, L., 2020. Cleaner approach to the recycling of metals in waste printed circuit boards by magnetic and gravity separation. J. Clean. Prod. 248, 119235. https://doi.org/10.1016/j.jclepro.2019.119235.

Web references

https://www.asus.com/Motherboards/EX-A320M-GAMING/. The last accessed time; 3.9.2020.
https://www.gigabyte.com/hr/Press/News/1283/. The last accessed time; 3.9.2020.